

## Leaf nitrogen estimation in potato based on spectral data and on simulated bands of the VENμS satellite

Y. Cohen · V. Alchanatis · Y. Zusman · Z. Dar · D. J. Bonfil ·  
A. Karnieli · A. Zilberman · A. Moulin · V. Ostrovsky ·  
A. Levi · R. Brikman · M. Shenker

Published online: 12 November 2009  
© Springer Science+Business Media, LLC 2009

**Abstract** Relationships between leaf spectral reflectance at 400–900 nm and nitrogen levels in potato petioles and leaves were studied. Five nitrogen (N) fertilizer treatments were applied to build up levels of nitrogen variation in potato fields in Israel in spring 2006 and 2007. Reflectance of leaves was measured in the field over a spectral range of 400–900 nm. The leaves were sampled and analyzed for petiole  $\text{NO}_3\text{-N}$  and leaf percentage N (leaf-%N). Prediction models of leaf nitrogen content were developed based on an optical index named transformed chlorophyll absorption reflectance index (TCARI) and on partial least squares regression (PLSR). Prediction models were also developed based on simulated bands of the future VENμS satellite (Vegetation and Environment monitoring on a New Micro-Satellite). Leaf spectral reflectance correlated better with leaf-%N than with petiole  $\text{NO}_3\text{-N}$ . The TCARI provided strong correlations with leaf-%N, but only at the tuber-bulking stage. The PLSR analysis resulted in a stronger correlation than TCARI with leaf-%N. An  $R^2$  of 0.95 ( $p < 0.01$ ) and overall accuracy of 80.5% (Kappa = 74%) were determined for both vegetative and tuber-bulking periods. The simulated VENμS bands

---

Y. Cohen (✉) · V. Alchanatis · Y. Zusman · V. Ostrovsky · A. Levi · R. Brikman  
Agricultural Research Organization, Volcani Center, Institute of Agricultural Engineering,  
Bet-Dagan, Israel  
e-mail: yafitush@volcani.agri.gov.il

Y. Zusman · M. Shenker  
The Seagram Center for Soil and Water Sciences, Hebrew University of Jerusalem, Rehovot, Israel

Z. Dar · A. Zilberman  
Extension Service, The Ministry of Agriculture, Bet-Dagan, Israel

D. J. Bonfil  
Field Crops and Natural Resources Department, Agricultural Research Organization,  
Gilat Research Center, Negev, Israel

A. Karnieli  
The Remote Sensing Laboratory, Jacob Blaustein Institutes for Desert Research, Ben Gurion  
University of the Negev, Sede-Boker Campus, Beersheba, Israel

A. Moulin  
Brandon Research Centre, Agriculture and Agri-Food Canada, Brandon, MB, Canada

gave a similar correlation with leaf-%N to that of the spectrometer spectra. The satellite has significant potential for spatial analysis of nitrogen levels with inexpensive images that cover large areas every 2 days.

**Keywords** Spectral reflectance · VENμS satellite · Transformed chlorophyll absorption in reflectance index (TCARI) · Partial least squares regression (PLSR) · Nitrogen · Potato

## Introduction

Potato (*Solanum tuberosum* L.) is an important crop worldwide, with total world production of about 360 million metric tons (National Potato Council (NPC) 2006). Potato is also becoming an important crop in Israel: in 2000 an area of 11 000 ha was seeded, which had increased to around 17 000 ha in 2005 (<http://www.cbs.gov.il/reader>). Potato yield and quality are very dependent on an adequate supply of nitrogen (Dar 2002; Errebhi et al. 1998). The relatively shallow root system of the potato crop, coupled with its large nitrogen (N) requirement and sensitivity to water stress on coarse textured soil increases the risk of nitrate ( $\text{NO}_3\text{-N}$ ) leaching. Therefore, precise N management for potato is important, both for maximizing production and for minimizing N loss to groundwater. Applying the right amount of N in the right place at the right physiological stage presents a challenge to potato growers, and matching fertilizer supply to the demands of the crop requires an adequate assessment of N status in the field. Potato growers usually apply more fertilizer N than is recommended as a safety measure because they do not want to sacrifice yield of a high-value crop when there are uncertainties about the accuracy of the recommended rates. There are few commercially available sensors to assess N status (Shock et al. 2007; Zebarth and Rosen 2007) or that account for spatial variability. The recent significant increase in nitrogen fertilizer costs has prompted efforts to devise strategies that will improve N use efficiency (NUE) in major crops such as potato. Previous research concluded that split applications of N to match potato growth needs would improve NUE considerably (e.g. Westermann and Kleinkopf 1985). In Israel potatoes are grown under irrigation, primarily on coarse sandy soil with a low organic content that is subject to N leaching when water and N are applied in excess (Alva 2008). Errebhi et al. (1998) showed that reducing the amounts of N applied at planting resulted in less  $\text{NO}_3\text{-N}$  leaching, greater N recovery by the crops and improved yield of marketable tubers. Meyer and Marcum (1998) demonstrated the need for pre-planting measurements of soil-N concentration to determine appropriate rates of N to apply. Dar (2002) suggested that the appropriate mid-season N rates and timing of application might be determined from petiole  $\text{NO}_3\text{-N}$  concentrations. Because of the temporal variability of soil N supply, strategies based on detecting crop N status at critical crop growth stages, and meeting crop N requirements with carefully timed fertilizer application might ultimately be more successful in improving NUE than those based on application at planting (Ferguson et al. 2002; Van-Alphen and Stoorvogel 2000). However, fertilizer management in irrigated potato production worldwide is currently based on uniform rates of N application and it does not take into account the spatial variation of plant N demand, which may result from within-field variability in soil and environmental characteristics. In the light of these considerations, there is considerable potential for varying the recommended timing and rates of N application according to petiole N level determined by measurements of soil and crop properties spatially distributed in the field at critical points of the growing season.

Remote sensing techniques can indicate crop N status (Al-Abbas et al. 1974; Botha et al. 2006; Gitelson et al. 2003; Thomas and Gausman 1977; Zakaluk and Ranjan 2007). Light reflected by vegetation in the visible region of the spectrum is predominantly influenced by chlorophyll pigments in the leaf tissues, and these relate to the leaf N concentration (Haboudane et al. 2002). Chlorophyll absorbs light in the red (~670 nm) and blue (~450 nm) portions of the spectrum (Gates et al. 1965), thereby providing diagnostic absorption features. In addition, near-infrared (NIR) reflectance is influenced by the internal structure of the leaf cell; well hydrated, healthy, spongy mesophyll cells reflect infrared wavelengths strongly (Gates et al. 1965). The spectral region between the red absorption feature and the region of high NIR reflectance, termed the 'red-edge', changes shape and position when the plant becomes deficient in N (e.g. Jain et al. 2007; Strachan et al. 2002). Therefore, measurements of reflected energy from crop leaves and canopies can be used to estimate chlorophyll concentration rapidly and provide a measure of N content (Haboudane et al. 2002; Jain et al. 2007).

The use of hyperspectral (HS) images, validated by ground-based spectral reflectance sensors, can address both spatial and temporal variability in leaf N content to improve mid-season N management. Hyperspectral images obtained by the Hyperion Satellite combine high spectral resolution with moderate spatial and temporal resolutions. In 2011, VENμS (Vegetation and Environment monitoring on a New Micro-Satellite) is to be launched (<http://smc.cnes.fr/VENUS>). VENμS is a joint research mission of the French Centre National d'Etudes Spatiales (CNES) and the Israel Space Agency (ISA). The system has spectral, spatial and temporal resolutions suitable for precision agriculture (PA), i.e. 12 narrow spectral bands (16–40 nm band width) in the visible and NIR ranges (420–910 nm); a ground resolution of 5.3 m and a 2-day revisit time (bands 5 and 6 have an identical range, which leaves 11 bands). Because of the unique combination of high spectral, spatial and temporal resolutions, and free availability of data during the first 2–4 years of operation, Venμs is expected to stimulate the adoption of PA concepts over large areas in conjunction with research into a variety of environmental conditions. The seven bands of the multi-spectral mode of the Compact Airborne Spectrographic Imager (CASI) are similar to some of the VENμS bands. Three of the CASI bands which have equivalents in the VENμS were used successfully to estimate chlorophyll content and to discriminate between N treatments in corn fields in Canada (Haboudane et al. 2002). The present paper describes part of an ongoing research project that aims to assess the potential of state-of-the-art multi-spectral and HS imaging technology for delineating management zones for variable-rate N application on potatoes. The objective of this study was to determine the relationships between spectral data and simulated bands of the VENμS satellite, and nitrogen levels in potato petioles and leaves.

## Materials and methods

The study was conducted in the spring growing seasons of 2006 and 2007 on two commercial potato fields planted with cv. Desiree in Kibbutz Ruhama, Israel (31.38°N, 34.59°E). This agricultural land is on the southern part of Israel's coastal plain, on the boundary between Mediterranean and semi-arid climates. The soil texture of both fields is sandy loam. The two fields follow a potato-wheat-sunflower or chickpea-wheat-potato crop rotation. Potato seed tubers were planted so that the hills (i.e. pairs of rows) were 1.93 m apart, and with a within-row spacing between plants of 0.2 m. The plots were planted at the beginning of February and harvested in mid-June. The average temperatures during this

**Table 1** Nitrogen treatments applied in the potato field in spring 2006

Nitrogen treatment	N rate (kg ha <sup>-1</sup> )	Percentage N rate relative to commercial rate	Application type
T100%	400	100	Commercial (urea); fertigation
T84%	335	84	Multigro <sup>®</sup> 43-0-0 SRN; base
T54%	215	54	Multigro <sup>®</sup> 43-0-0 SRN; base
T25%	100	25	Multigro <sup>®</sup> 43-0-0 SRN; base
T0%	0	0	Base

**Table 2** Nitrogen treatments applied in the potato field in spring 2007

Nitrogen treatment	N rate (kg ha <sup>-1</sup> )	Percentage N rate relative to commercial rate	Application type
T100%	400	100	Commercial (urea); fertigation
T75%	300	75	Multigro <sup>®</sup> 43-0-0 SRN; base
T50%	200	50	Multigro <sup>®</sup> 43-0-0 SRN; base
T25%	100	25	Multigro <sup>®</sup> 43-0-0 SRN; base
T0%	0	0	Base

period were between 15 and 35°C. The average annual rainfall during the spring season in this region is only 100 mm, therefore the fields were irrigated. In both seasons the plots received the same applications of pre-season compost (30 m<sup>3</sup> ha<sup>-1</sup>), phosphate (180 kg ha<sup>-1</sup>) and KCl (180 kg ha<sup>-1</sup>).

To assess the N status of potatoes, five N treatments with four replicates were applied in each season. In 2006 an area of 1.2 ha was divided into 20 sub-plots of 5 × 120 m. In 2007, to enable the recognition and analysis of the sub-plots in airborne hyperspectral images, an area of 8 ha was divided into sub-plots of 18 × 50–100 m. The treatments in both seasons included commercial treatment (fertigation) with N (supplied as urea) at 400 kg N ha<sup>-1</sup>. In the first year four reduced rates of N were applied, 0, 100, 215 and 335 kg N ha<sup>-1</sup>, and in the second year the rates were changed to 0, 100, 200 and 300 kg N ha<sup>-1</sup>. In both years the reduced N treatments were applied as a slow release coated urea granular fertilizer (Multigro 43-0-0 SRN, Haifa Chemicals Inc., Haifa, Israel) at a single application before planting (Tables 1 and 2).

### Spectral data collection

Reflectance of leaves in the field was measured with an HR2000 mini-spectrometer (OceanOptics Inc., Dunedin, FL, USA) with a spectral range of 400–900 nm and a 50-μm slit. The optical spectral resolution of the system, determined by the slit width and the diffraction grating, was 1.8 nm (full width at half maximum, FWHM). The spectrometer was equipped with a 2048-pixel silicon based array, with a signal-to-noise ratio of 250:1 and connected to a laptop computer. An LS-1halogen light source (Ocean Optics Instrument, OOI), in combination with a fiber optic reflectance probe were used to illuminate the leaf and to collect the reflected light. The reflectance probe consisted of six 400 μm diameter optical fibers arranged in a circle to illuminate the sample, and a sensing fiber

**Table 3** Summary of measurement dates and available spectral and ground truth data

	Days after planting	Spectral measurements	Petiole NO <sub>3</sub> -N analysis	Total %N in leaves
2006	50	✓	✓	Not measured
	78	Corrupted	✓	Not measured
	92	✓	✓	Not measured
	99	✓	✓	Not measured
2007	55	✓	✓	✓
	69	✓	✓	✓
	82	✓	✓	✓
	97	✓	✓	✓

which transferred the reflected light to the spectrometer. A sampling cell was designed and constructed to conduct leaf reflectance measurements in the field. The sampling cell shielded the sampled leaf against ambient light, and maintained a constant distance of 10 mm between the leaf sample and the reflection probe (Alchanatis et al. 2005). The integration time was 1500 ms, with an average of three spectra per acquisition. White and dark reference signals were sampled at the beginning of each plot.

Field observations were made on four days in each of the two seasons. On each day, spectral reflectance was measured in the youngest fully expanded leaf of each of 20 plants from each of the two replicates of each N treatment. These leaves were sampled and NO<sub>3</sub>-N was measured in five 4-petiole groups for each of the sampled sub-plots. In 2007 leaves were analyzed for leaf-%N also.

The spectral data from the second acquisition date in 2006 were found to be corrupted and were not used for further analysis. Table 3 summarizes the measurement dates and the available spectral and ground truth data.

### Spectral data analysis

Prediction models of N levels were developed by three methods:

1. Calculation of the transformed chlorophyll absorption reflectance index (TCARI),
2. Partial least squares regression (PLSR) analysis of the whole spectrum,
3. Simulation of the VENμS bands, followed by TCARI calculation and multivariate linear regression (MLR) analysis of the simulated bands.

### Calculation of TCARI

Many vegetation indices (VIs) have been developed to estimate crop biophysical parameters and various stresses. The majority of the VIs developed for assessing N content in vegetation are based on indirect indicators of chlorophyll content (Daughtry et al. 2000). These indices, can be grouped into two categories, namely, chlorophyll related indices such as the chlorophyll vegetation index (CVI) and the CARI family; and the red edge indices which are essentially a ratio between reflectance of two bands in the the red-edge range such as the ratio 740 and 720 ( $\rho_{740}:\rho_{720}$ ). From proposed indices in the literature (e.g. Jain et al. 2007 and Vincini and Frazzi 2009) TCARI was shown to be an effective

leaf chlorophyll estimator (Vincini and Frazzi 2009). Therefore, we selected TCARI to represent the VI approach in this study. The equation for TCARI introduced by Haboudane et al. (2002) is given by

$$TCARI = 3 \left[ (\rho_{700} - \rho_{670}) - 0.2(\rho_{700} - \rho_{550}) \left( \frac{\rho_{700}}{\rho_{670}} \right) \right], \quad (1)$$

where  $\rho$  is the reflectance value of the corresponding wavelength. The TCARI is a modification of the modified chlorophyll absorption reflectance index (MCARI) that was developed by Daughtry et al. (2000):

$$MCARI = [(\rho_{700} - \rho_{670}) - 0.2(\rho_{700} - \rho_{550})] \left( \frac{\rho_{700}}{\rho_{670}} \right). \quad (2)$$

According to Gitelson and Merzlyak (1997), wavelengths in the range 530–630 nm and of 700 nm are sensitive to the chlorophyll content in plant leaves. The 550 nm band matches the minimum chlorophyll absorption in the visible region (Haboudane et al. 2002); therefore the MCARI comprises one chlorophyll absorption band at 670 nm and two chlorophyll-sensitive bands at 550 and 700 nm. The MCARI was applied to corn (Daughtry et al. 2000; Haboudane et al. 2002, 2004), wheat and soybean (Haboudane et al. 2004). The TCARI is calculated from the same bands as the MCARI, but the ratio between the reflectance at 700 and 670 nm is used to filter the background reflectance at 700 and 550 nm. To differentiate further between LAI and chlorophyll sensitivity Haboudane et al. (2002) proposed the ratio of TCARI:OSAVI, where the optimized soil adjusted vegetation index (OSAVI, Rondeaux et al. 1996) is introduced to minimize the sensitivity to differences in the canopy LAI:

$$\frac{TCARI}{OSAVI} = \frac{3 \left[ (\rho_{700} - \rho_{670}) - 0.2(\rho_{700} - \rho_{550}) \frac{\rho_{700}}{\rho_{670}} \right]}{\frac{1.16 (\rho_{800} - \rho_{670})}{\rho_{800} + \rho_{670} + 0.16}}. \quad (3)$$

Hu et al. (2004) predicted chlorophyll content successfully from airborne sensor measurements by applying the TCARI:OSAVI ratio to corn, soybean and wheat fields. Zarco-Tejada et al. (2005) compared chlorophyll estimates of vines obtained with TCARI and with TCARI:OSAVI; they found TCARI advantageous for pure vegetation data and TCARI:OSAVI for mixed soil and vegetation data. Vincini and Frazzi (2009) showed that TCARI:OSAVI and the CVI (Vincini et al. 2008) resulted in stronger correlations with chlorophyll concentration in the canopy level than those for the red-edge based indices. When applied to potato, both TCARI and TCARI:OSAVI were insensitive to changes in N content in the canopy level (Jain et al. 2007; Herrmann et al. 2009). TCARI:OSAVI was found sensitive to changes in N content in potato canopy when band 670 nm was replaced with band 1505 nm (Herrmann et al. 2009).

In the present study a regression model that linked the means of replicate data of TCARI and leaf N levels was calculated for 66% of the data, leaving 34% of the data to be used for validation. The regression model was applied to the entire data set.

#### *Partial least squares regression (PLSR)*

This analysis is a chemometric technique that generalizes and combines the methods of principal component analysis (PCA) and multiple regression; it is used to predict a set of dependent variables from a large set of independent ones (i.e. predictors) that may be

correlated. The PLSR analysis has enabled N status in wheat and corn to be predicted from ground-based spectral data (Alchanatis et al. 2005; Bonfil et al. 2005) and in forests from hyperspectral images (Coops et al. 2003; Ollinger et al. 2002; Smith et al. 2002; Townsend et al. 2003). The PLSR analysis of spectra is based on the statistical analysis of wavelengths from a wide spectrum, in contrast to linear regression for indices such as TCARI. It exploits the whole length of the spectrum by forming predictive models of the constituent concentration data, e.g. N concentration, based on a few extracted factors (components or latent variables (LVs)) (Shenk and Westerhaus 1991). As a result, wavelength loadings for significant PLSR factors, from which regression coefficients are derived, are related directly to concentrations of constituents. The PLSR factors also describe the spectral variation most relevant to modeling the chemical variation. In the present study, the independent variables for PLSR analysis were the raw spectra and the first-derivatives (see below) of the reflectance spectra over the whole measured range (400–900 nm). They were used to predict both petiole  $\text{NO}_3\text{-N}$  and leaf-%N. By contrast to the TCARI analysis, which was based on means of replicate data, the data from all sites were used as input for PLSR analysis. Thus, for petiole  $\text{NO}_3\text{-N}$  there were 350 samples (50 from each of seven dates from both 2006 and 2007), and for leaf-%N there were 200 samples (50 from each of four dates from 2007 only) (Table 3). The first derivative was calculated for a given wavelength as the slope of smoothed reflectance (Savgol smoothing in a 15 nm window). The use of first derivative spectra provided an alternative for identifying the actual absorbance features that form the physical basis for identifying N concentration through spectroscopy. Specifically, the first derivative identifies differences between the slopes of the spectra, meaning that absorbance features related to canopy chemistry are identified from relative differences in the linear rate of change of reflectance within a given wavelength region. As a consequence, the actual bands identified as being related to N concentration may not be centered on wavelengths known to exhibit absorbance features, but rather on those adjacent to known absorbance features. In addition, the use of the first derivative enables baseline offsets of intensity and low-frequency variations to be removed or substantially minimized (Smith et al. 2002). The PLSR models were calibrated and cross validated with the PLS Toolbox (Eigenvector Research Inc., Wenatchee, WA, USA) and MATLAB software (The MathWorks, Natick, MA, USA). The performances of the models were evaluated by a full leave-one-out cross validation. This process calibrated the PLSR models iteratively using all the data except for one. In each iteration, a different sample was left out from the data until every sample had been left out once. Values for samples left out of the calibration were then predicted and the prediction residuals were computed. All prediction residuals were combined to calculate the cross-residual variance. The number of latent variables for each model was selected by choosing the number that resulted in the smallest root mean squared error of cross validation (RMSECV). The measured and predicted N values were then averaged for each replication and the RMSECV was recalculated and used as an indication of the average model error.

#### *Simulation of VEN $\mu$ S satellite bands, TCARI calculation and MLR analysis*

Based on the spectrometer data, we simulated 10 out of 11 VEN $\mu$ S bands (Table 4), taking into account the equivalent central wavelength (nm) and band-width. The theoretical spectral response of each VEN $\mu$ S band was overlaid with the actual spectral reflectance curve obtained from the spectrometer. The TCARI was calculated by Eq. 1 where bands

**Table 4** VEN $\mu$ S multispectral camera bands

Band number	Equivalent central wavelength (nm)	Band-width (nm)	Region
1	420	40	Blue
2	443	40	Blue
3	490	40	Green
4	555	40	Green
5–6	620	40	Red
7	667	30	Red edge
8	702	24	Red edge
9	742	16	Red edge
10	782	16	NIR
11	865	40	NIR
12 <sup>a</sup>	910	20	NIR

<sup>a</sup> Band 12 was not simulated because the spectral range measured was 400–900 nm

550, 670 and 700 nm were shifted with the simulated VEN $\mu$ S bands 555, 667 and 702, respectively. Since there are only 10 VEN $\mu$ S bands, MLR analysis rather than PLSR was applied. The MLR was applied to data from all sites for all dates. The measured and the predicted N values were then averaged for each replication and the RMSECV was used as an indication of the average model error.

#### Analysis of classification accuracy

In addition to the RMSECV, the quality of the models was evaluated based on their ability to classify nitrogen content into pre-defined nitrogen ranges. Such a classification is suitable for the future use of such models to support decisions on variable-rate applications. The accuracy of classification was determined with the Kappa coefficient for four classes of measured and predicted petiole NO<sub>3</sub>-N and leaf-%N values, which represented a reasonable number of possible variable application rates. The classes were based on intervals of 250 mg kg<sup>-1</sup> and 0.5% for petiole NO<sub>3</sub>-N and leaf-%N, respectively (Table 5).

A confusion matrix was formed to calculate the Kappa coefficient of agreement ( $k$ ) for each model in which the principal diagonal entries reflected the correct classification. The proportion of the total number of instances correctly classified among the total number of instances represented the ‘overall accuracy’ of the classification. The coefficient  $k$  was calculated by Eq. 4 based on overall accuracy and the proportion of units expected by chance agreement (Tso and Mather 2001):

$$k = \frac{N \sum_{i=1}^r X_{ii} - \sum_{i=1}^r (x_{i+} \times x_{+i})}{N^2 - \sum_{i=1}^r (x_{i+} \times x_{+i})}, \quad (4)$$

where  $r$  is the number of rows in the confusion matrix,  $X_{ii}$  is the number of combinations along the principal diagonal,  $x_{i+}$  is the total number of observations in row  $i$ ,  $x_{+i}$  is the total number of observations in column  $i$  and  $N$  is the total number of instances. In addition, the percentages of incorrect classifications to adjacent classes were calculated on two or three levels of proximity, i.e. high cost errors.



**Table 5** Petiole  $\text{NO}_3\text{-N}$  and leaf-%N classes

N level	Petiole $\text{NO}_3\text{-N}$ range ( $\text{mg kg}^{-1}$ )	Leaf-%N range
1	<250	<3.5
2	250–500	3.5–4.0
3	500–750	4.0–4.5
4	>750	4.5–5.0

## Results

### Temporal changes in N levels and yield variables

Petiole  $\text{NO}_3\text{-N}$  decreased during the growing season for all fertilizer treatments. When petiole  $\text{NO}_3\text{-N}$  data for day 50 after planting in 2006 are compared with optimal, excess and deficient guidelines (Dar, 2002) (Fig. 1a), means for all treatments are close to the optimum value with the exception of the ‘no-N’ treatment (T0%). On all other days, petiole  $\text{NO}_3\text{-N}$  levels of T100%, T84% and T54% are above the excess guideline, whereas for T25% and T0% they are below the deficit.

The 2007 data (Fig. 1b) show that similar temporal changes occurred, but with a few differences. Although T100% and T75% values are close to the optimum guideline or above the excess at all dates, those for T25% and T0% are close to or below the deficit. Petiole  $\text{NO}_3\text{-N}$  concentrations for T50% are close to the optimal level on the first three dates, but are below the deficit on the last date, i.e. 97 days after planting, and those for T25% and T0% behave similarly.

Potato yield and the percentage of large tubers were assessed for each treatment in each year of the study (Fig. 2). With the slow-release N formulations, yield quantity and quality increases with increasing N content. It reaches maximum values at an application rate of around 50%, with no significant differences ( $p < 0.05$ ) from the values for T84% in 2006 and T75% in 2007. Nevertheless, both yield variables are slightly less for T84% than for T54% in 2006, whereas in 2007 those for T75% are slightly larger than those in the latter two. The commercial fertigation treatment, T100%, elicited different responses in each season: in 2006 its values are similar to those for T54% and larger than those for T84%, whereas in 2007 T100% gives smaller values than either T50% or T75%.

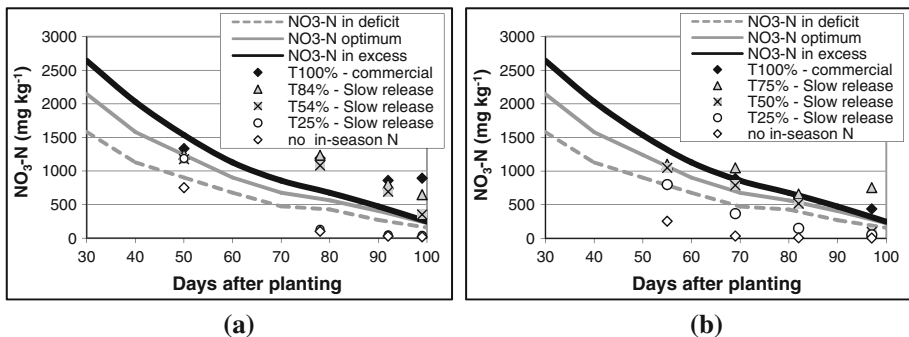


**Fig. 1** Petiole  $\text{NO}_3\text{-N}$  content in the youngest fully expanded leaves of plants from the five N treatments for the growth period in: **a** 2006 and **b** 2007, compared to the optimal, excess and deficit guidelines for petiole  $\text{NO}_3\text{-N}$  in potato, ‘Desiree’, for the spring season. Each data point is the average of five 4-petiole groups for each of the sampled sub-plots

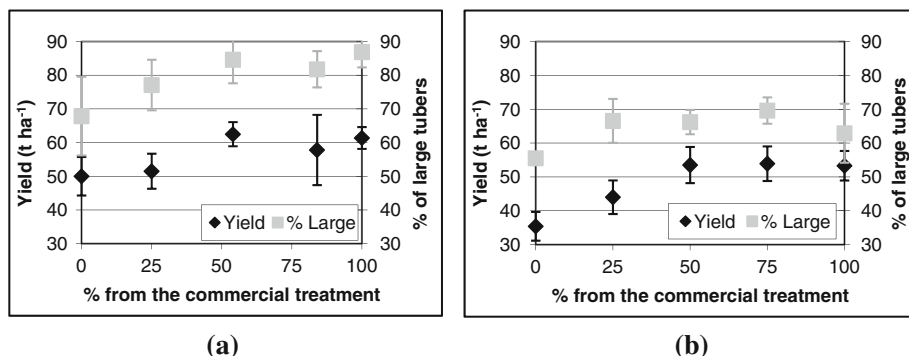
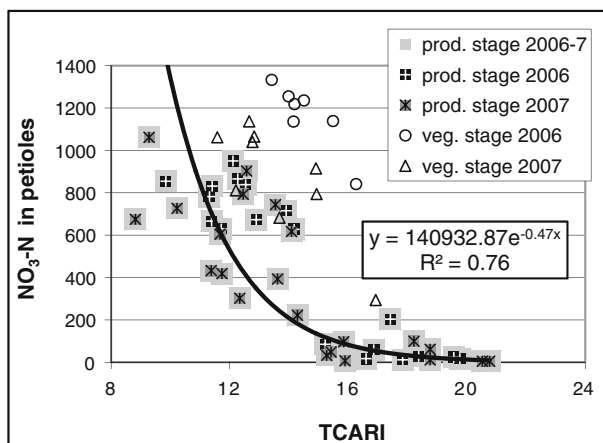


**Fig. 2** Yield quantity and percentage of large tubers for each treatment in: **a** 2006 and **b** 2007. The bars represent  $\pm 1$  standard deviation values

### Relationships between TCARI and N levels

Petiole  $\text{NO}_3\text{-N}$  content, leaf-%N and TCARI values were averaged among replicates. All petiole  $\text{NO}_3\text{-N}$  contents from all dates in the two spring seasons were plotted against TCARI values (Fig. 3). The vegetative stage (data from 50–55 days after planting) and the subsequent production stage (the tuber-bulking period, i.e. from 60 to 100 days after planting) are shown separately. The 'TCARI -  $\text{NO}_3\text{-N}$ ' relationships for data from the vegetative stage are different from the data of the tuber-bulking period. For the first period, there are different negative linear models for each season. By comparison, there is a single negative non-linear relationship for the tuber-bulking period for both seasons. The RMSECV is  $326 \text{ mg kg}^{-1}$ , which is about 30% of the range of petiole  $\text{NO}_3\text{-N}$  content ( $0\text{--}1100 \text{ mg kg}^{-1}$ ). Moreover, the non-linear model provides a qualitative separation between the two main levels of petiole  $\text{NO}_3\text{-N}$  content, i.e. less than and more than  $250 \text{ mg kg}^{-1}$ . This binary division showed an overall accuracy of 90% ( $n = 41$ ). The confusion matrix for four groups is given in Table 6. It shows that when the  $\text{NO}_3\text{-N}$  content was classified into four levels, the overall accuracy reduces to 61% ( $p < 0.01$ ) with a Kappa coefficient of 41.5%. In addition, there are 19.5% ( $n = 8$ ) of high cost errors.

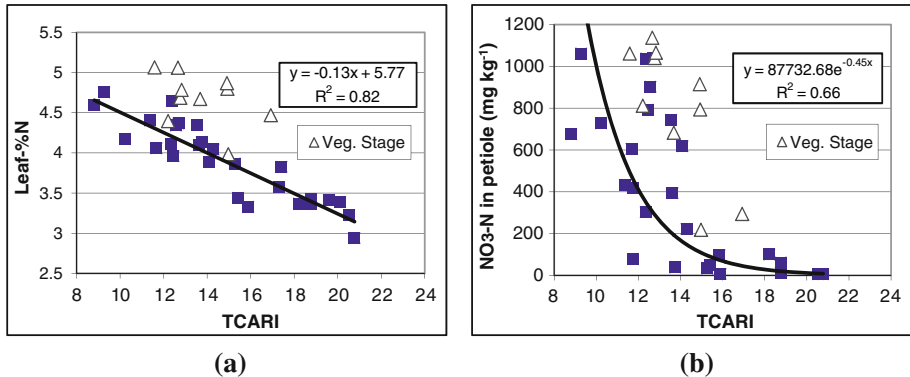
**Fig. 3**  $\text{NO}_3\text{-N}$  as a function of TCARI values from all dates in both seasons. *Veg. stage* and *prod. stage* relate to the vegetative stage and the production stage, respectively



**Table 6** Confusion matrix between measured and predicted petiole  $\text{NO}_3\text{-N}$  values based on the TCARI model

	Measured petiole $\text{NO}_3\text{-N}$ ( $\text{mg kg}^{-1}$ )	Predicted petiole $\text{NO}_3\text{-N}$ ( $\text{mg kg}^{-1}$ )			
		<250	250–500	500–750	>750
	<250	19			
	250–500	1	1	2	
	500–750	3	2	3	1
	>750		5	2	2

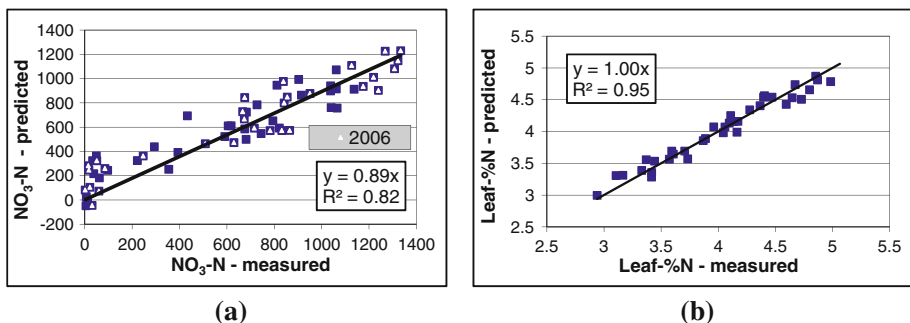
Overall accuracy  $25/41 = 61\%$   
 high cost errors (in *italics*)  $8/41 = 19.5\%$

**Fig. 4** **a** Leaf-%N and **b** petiole  $\text{NO}_3\text{-N}$  as a function of TCARI values for all sampling dates in 2007

The correlation between TCARI and leaf-%N is stronger for the 2007 data. Figure 4a shows that, when data from the first date were excluded, the relationship between TCARI and leaf-%N is a negative linear one. For comparison, Fig. 4b shows the scatter plot of TCARI against  $\text{NO}_3\text{-N}$  for 2007. The RMSECV of 'TCARI - leaf-%N' was 0.2%, which is 10% of the range of leaf-%N (2.9–4.8%). The overall accuracy and Kappa coefficient were 81% ( $p < 0.01$ ) and 72.5%, respectively, with no high cost errors ( $n = 26$ ).

#### Partial least squares regression (PLSR) analysis

Prediction models were developed by analyzing the raw reflectance data and their first derivative by PLSR; both gave similar results. The PLSR analysis results in prediction

**Fig. 5** Measured against predicted: **a**  $\text{NO}_3\text{-N}$  in 2006–2007 and **b** leaf-%N in 2007 based on PLSR analysis

models of petiole  $\text{NO}_3\text{-N}$  with  $R^2 = 0.82$  ( $n = 64$ ;  $p < 0.01$ ) for all data from all dates in both seasons (Fig. 5a). The best prediction model for reflectance was determined with ten latent variables (factors), and the first derivative was calculated with only five. The RMSECVs of both models were  $164 \text{ mg kg}^{-1}$ , or 12% of the range of petiole  $\text{NO}_3\text{-N}$  content ( $0\text{--}1100 \text{ mg kg}^{-1}$ ). This is an improvement of 50% over the TCARI-based model. The overall classification accuracy for four groups and the Kappa coefficient were 70 and 59%, respectively, with no high cost errors.

The correlation between spectral data and leaf-%N values for the model developed with PLSR is stronger (Fig. 5b;  $R^2 = 0.95$ ,  $n = 36$ ;  $p > 0.01$ ) than for  $\text{NO}_3\text{-N}$  content. The RMSECV was 0.11%, i.e. 5% of the range of leaf-%N values ( $2.9\text{--}5.1\%$ ). Overall classification accuracy and the Kappa coefficient were 80.5 and 74%, respectively, with no high cost errors.

### Analysis of simulated $\text{VEN}_{\mu\text{S}}$ bands

The petiole  $\text{NO}_3\text{-N}$  and leaf-%N were analyzed by TCARI which was calculated from three of the simulated  $\text{VEN}_{\mu\text{S}}$  bands, and also by MLR applied to all spectral bands. The

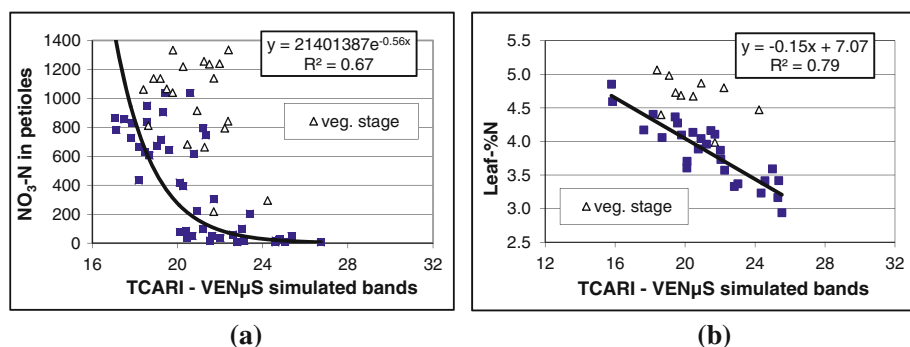


**Fig. 6** **a**  $\text{NO}_3\text{-N}$  in 2006–2007 and **b** leaf-%N in 2007 as a function of TCARI values using the simulated  $\text{VEN}_{\mu\text{S}}$  bands. *Veg. stage* relates to the vegetative stage

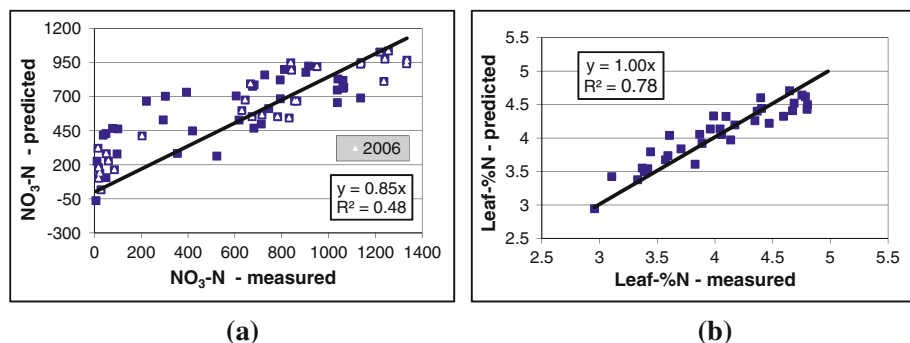


**Fig. 7** Measured against predicted: **a**  $\text{NO}_3\text{-N}$  in 2006–2007 and **b** leaf-%N in 2007 based on MLR analysis of the simulated  $\text{VEN}_{\mu\text{S}}$  bands petiole

relationships between TCARI based on the VEN $\mu$ S simulated bands and petiole NO<sub>3</sub>-N and leaf-%N (Fig. 6a and b) are similar to their equivalents based on the original narrow bands of the spectrometer data (Fig. 4a and b). The relationship between TCARI and leaf-%N is similar ( $R^2 = 0.79$ ;  $n = 27$ ;  $p < 0.01$ ; RMSECV = 11%), but the accuracy was less when four classes were used (overall accuracy of 70% and Kappa of 57%).

The MLR models calculated from the simulated VEN $\mu$ S bands give inferior results to those of similar models based on the original spectral data. The correlation with petiole NO<sub>3</sub>-N content is weak ( $R^2 = 0.48$ ;  $n = 64$ ), with an RMSECV of 230.7 mg kg<sup>-1</sup> (17% of the overall range, Fig. 7a). Furthermore, the accuracy of the overall petiole NO<sub>3</sub>-N classification and Kappa coefficient were only 61 and 46%, respectively, with 2% of high-cost errors.

By contrast, leaf-%N is strongly correlated with the simulated bands (RMSECV = 0.2, 10% of the overall range, Fig. 7b). The overall classification accuracy and Kappa coefficient are 60 and 46%, respectively, with no high cost errors.

## Discussion

Stable calibration models need comprehensive data that cover several seasons (Bonfil et al. 2005, Pimstein et al. 2007). The main objective of this study was to test the feasibility of determining the relationships between leaf spectral reflectance and simulated bands of the VEN $\mu$ S satellite, and nitrogen levels in potato petioles and leaves. Two seasons were used in this study for model calibration and cross validation. Table 7 summarizes the performance measures of all types of analysis. Leaf-%N was more strongly correlated with

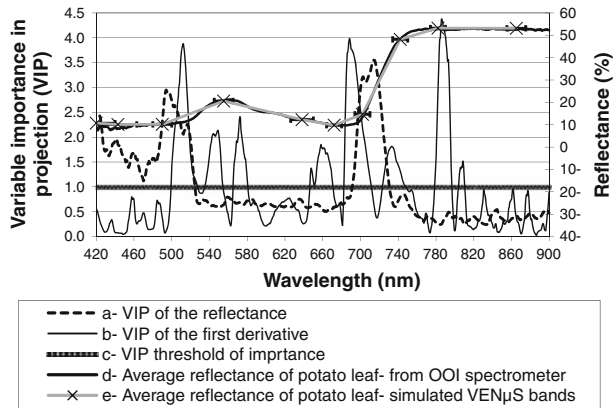
**Table 7** Accuracy indices for the various types of data analyses

Data type	Nitrogen measure and season	Analysis technique	$R^2$	RMSECV (%)	Overall accuracy (%)	Kappa (%)	High cost errors (%)	Phenological stage
Original spectra	Petiole NO <sub>3</sub> -N content 2006–2007	TCARI	0.76 <sup>a</sup> $n = 41$	30	61	40.5	19.5	prod.
		PLSR	0.82 $n = 65$	12	70	59	0	veg. + prod.
	Leaf-%N-2007	TCARI	0.80 $n = 26$	10	81	72.5	0	prod.
		PLSR	0.95 $n = 36$	5	80.5	74	0	veg. + prod.
Simul-ated VEN $\mu$ S bands	Petiole NO <sub>3</sub> -N content 2006–2007	TCARI	0.67 $n = 44$	29	61	40	14	prod.
		MLR	0.48 $n = 64$	17	61	46	2	veg. + prod.
	Leaf-%N-2007	TCARI	0.79 $n = 27$	11	70	57	0	prod.
		MLR	0.78 $n = 35$	10	60	46	0	veg. + prod.

veg. and prod. relate to the vegetative stage and the production stage, respectively

<sup>a</sup> All  $R^2$  are significant at  $p < 0.05$

**Fig. 8** The VIP of PLSR models based on: *a* the reflectance and *b* the first derivative; *c* VIP threshold of significant importance; average reflectance of a potato leaf based on: *d* the original spectra and *e* on VEN $\mu$ S simulated bands. The horizontal bars represent the band width of the VEN $\mu$ S bands



spectral data than petiole  $\text{NO}_3\text{-N}$ . This might be because petiole  $\text{NO}_3\text{-N}$  reflects N status in the short term, whereas leaf-%N represents it in the longer term. The TCARI was moderately correlated with leaf-%N, but this was limited to the tuber-bulking stage. The use of the full measured spectrum (400–900 nm) with PLSR analysis increased the accuracy of estimated N levels compared with the use of TCARI using a few selected bands. In addition, and in contrast to the TCARI results, a single model could apply to both the vegetative and the tuber-bulking periods. Furthermore, PLSR analysis achieved greater accuracy in terms of all performance measures.

### PLSR versus TCARI

The relative importance of spectral wavelengths can be determined by PLSR analysis. The relative importance of each wavelength can be evaluated according to the variable importance in projection (VIP) of the independent variables. In general, a VIP value larger than one unit indicates that the contribution of that wavelength is significant, and the larger the VIP value, the greater is the contribution of that wavelength to the model. Despite the differences between the VIP values obtained by PLSR analysis of the raw reflectance data (Fig. 8a) and of the first derivatives (Fig. 8b), two expected ranges can be observed: 450–530 and 680–730 nm. The first range features rapid change from relatively low reflectance in the blue range to greater reflectance in the green range (Fig. 8c); the second range straddles the red edge (Fig. 8c). The spectra in the 450–530 nm range are strongly influenced by the presence and abundance of chlorophyll (Gates et al. 1965; Townsend et al. 2003). By contrast, the spectra in the 680–730 nm range may be correlated with internal leaf structure also. In the relatively limited spectral range measured in the present study, these were the spectral ranges that could be indirectly related to nitrogen content. These results are consistent with those of studies that analyzed hyperspectral images with PLSR for estimating N concentrations in forests (Coops et al. 2003; Smith et al. 2002).

Within these two ranges of wavelengths, large VIP scores (of the raw spectra and the first derivative) were obtained for the TCARI bands. The large VIP scores for a wider range around these bands showed the importance of the gradual change in reflectance for predicting leaf-%N. Thereby, the predictive potential of PLSR analyses of spectra is greater than that for indices such as TCARI.

### Spectrometer reflectance versus simulated VEN $\mu$ S bands:

The simulated VEN $\mu$ S bands performed similarly to the full width spectra for predicting leaf-%N. However, the accuracy was much less than for the prediction of petiole NO<sub>3</sub>-N content. Five of the 11 simulated VEN $\mu$ S bands are in the two important transition zones (bands 3–4 and 7–9, Table 4), a position that enables them to be used to evaluate leaf-%N. However, there are far fewer VEN $\mu$ S bands and they are wider (Fig. 8e). Thereby the VEN $\mu$ S bands may describe a significant part of the differences in the transition zones, but their use may not be as accurate as that of the whole spectrum.

**Fig. 9** The TCARI based on the original narrow bands against TCARI based on the simulated VEN $\mu$ S bands (data from 2007)

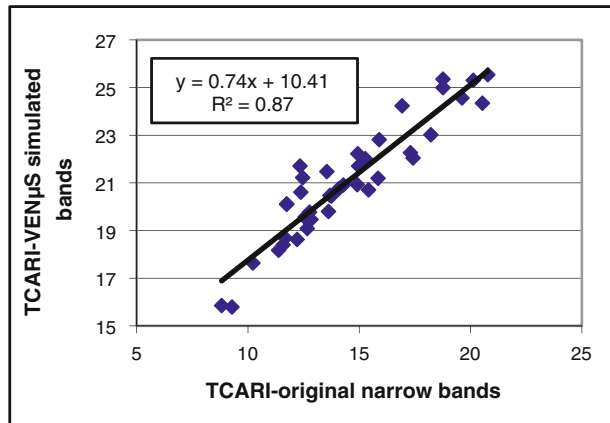
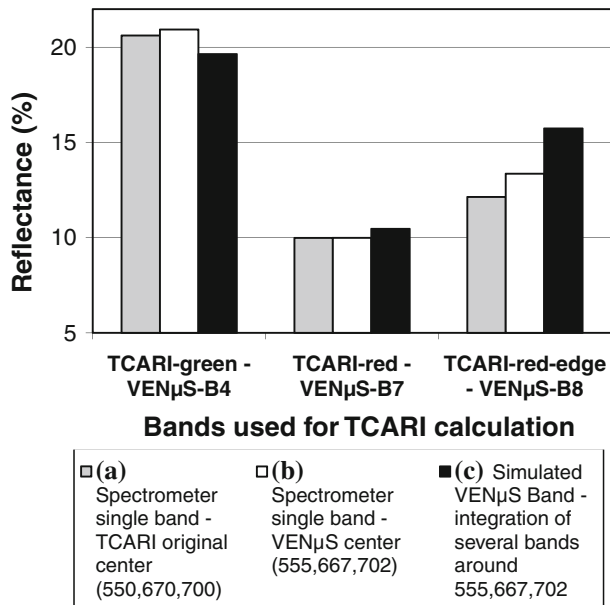


**Fig. 10** Reflectance of original TCARI bands from the spectrometer (a), as related to the center (b) and as related to the width of the simulated VEN $\mu$ S bands (c). For more detail see Table 4



### TCARI

Comparison of two TCARI-based models for prediction of leaf-%N, one based on narrow-bands from the intensive spectral data of the spectrometer (Fig. 4a) and one on broad bands from the simulated VEN $\mu$ S bands (Fig. 6b), shows the importance of the wavelengths and distribution of the VEN $\mu$ S bands. The two models have similar slopes ( $-0.13$  and  $-0.15$ ), but have different intercepts. This is attributed to a shift of the TCARI values when they are calculated for the simulated VEN $\mu$ S bands (Fig. 9). Despite the expected strong correlation between the two sets of TCARI values (Fig. 9), the TCARI values derived from the simulated VEN $\mu$ S bands are significantly ( $p < 0.001$ ) larger than those based on the original spectral data. The 550- and 700-nm bands of the TCARI are in the transition zones of typical leaf spectra (Fig. 8d and e), and the equivalent VEN $\mu$ S bands for TCARI are not identical to the original central bands, as indicated by Haboudane et al. (2002) (Eq. 1, Table 4). Also, the VEN $\mu$ S bands are much wider than the bands of the spectrometer. Both modifications contribute to the differences in reflectance of the TCARI bands, especially in transition zones such as the red-edge range (Fig. 10). These differences resulted in significantly different TCARI values, which changed the intercept of the prediction model.

### MLR analysis

When all simulated VEN $\mu$ S bands are analyzed by MLR the differences mentioned above in reflectance may be enhanced, as can be seen in the results derived from the PLSR models of the intensive spectral data, the MLR models of the simulated VEN $\mu$ S bands, and their accuracies (Table 7; Figs. 5 and 7).

### Conclusions

The results of this study demonstrate both the need for continuous monitoring of leaf nitrogen levels in potato fields and the potential of the use of spectral indices and sensors for this purpose. The TCARI for single leaves in the field was strongly correlated with potato petiole NO $_3$ -N and leaf-%N. A model based on PLSR of the spectrum in the 400–900 nm range was strongly correlated with petiole NO $_3$ -N and leaf-%N during the vegetative and tuber-bulking periods. The correlation of simulated VEN $\mu$ S spectra with leaf-%N was similar to that of the spectra obtained from the spectrometer. However, the correlation was weaker with respect to petiole NO $_3$ -N. The VEN $\mu$ S satellite has considerable potential for mapping spatio-temporal changes in leaf-%N since it can provide images of large areas every 2 days at low cost. However, in Israel (and also in other countries, e.g. the USA and Canada) decisions on fertilizer application in potato fields during the course of the season are based on petiole sampling and chemical analysis for NO $_3$ -N content, which is relatively quick and cheap. The 2007 data show that the correlation between petiole NO $_3$ -N and leaf-%N was statistically significant but moderate ( $r^2 = 0.63$ ). Our future research will investigate aerial HS images that were taken above the experimental fields and assess the correlation of simulated VEN $\mu$ S images (rather than bands only) with the spatial variation of N levels in potato fields. If aerial HS images and/or simulated VEN $\mu$ S images were strongly correlated with the spatial variation of leaf-%N or



plant-%N and not with petiole  $\text{NO}_3\text{-N}$ , then additional research would be required to relate petiole  $\text{NO}_3\text{-N}$  content or decisions on N fertilizer application to leaf-%N and or plant-%N.

**Acknowledgments** This project was supported by the Israeli Space Agency, Israeli Ministry of Science and also by Research Grant Award No. CA-9102-06 from BARD-AAFC—The United States—Israel Binational Agricultural Research and Development Fund and Agriculture and Agri-Food, Canada. The authors wish to express their appreciation of the vital contributions of Gadi Hadar and Ran Ferdman, potato growers from Kibbutz Ruhama, who provided land, seed and pesticide, and managed the irrigation for the project at no cost. The field experiments could not have been performed without the collaboration of Yossi Sofer from Haifa Chemicals, Ltd. We are also grateful for the anonymous reviewers for their constructive remarks.

## References

- Al-Abbas, A. H., Barr, R., Hall, J. D., Crane, F. L., & Baumgardner, M. F. (1974). Spectra of normal and nutrient-deficient maize leaves. *Agronomy Journal*, 66, 16–20.
- Alchanatis, V., Schmilovitch, Z., & Meron, M. (2005). In-field assessment of single leaf nitrogen status by spectral reflectance measurements. *Precision Agriculture*, 6, 25–39.
- Alva, K. A. (2008). Water management and water uptake efficiency by potatoes: A review. *Archives of Agronomy and Soil Science*, 54, 53–68.
- Bonfil, D. J., Karnieli, A., Raz, M., Mufradi, I., Asido, S., Egozi, H., et al. (2005). Rapid assessing of water and nitrogen status in wheat flag leaves. *Journal of Food Agriculture and Environment*, 3, 148–153.
- Botha, E. J., Zebarth, B. J., & Leblon, B. (2006). Non-destructive estimation of potato leaf chlorophyll and protein contents from hyperspectral measurements using the PROSPECT radiative transfer model. *Canadian Journal of Plant Science*, 86, 279–291.
- Coops, N. C., Smith, M. L., Martin, M. E., & Ollinger, S. V. (2003). Prediction of eucalypt foliage nitrogen content from satellite-derived hyperspectral data. *IEEE Transactions on Geoscience and Remote Sensing*, 41, 1338–1346.
- Dar, Z. (2002). *Potato crop protocol*. Bet Dagan, Israel: Ministry of Agriculture Extension Service. in Hebrew.
- Daughtry, C. S. T., Walthall, C. L., Kim, M. S., Brown de Colstoun, E., & McMurtrey, J. E. (2000). Estimating corn leaf chlorophyll concentration from leaf and canopy reflectance. *Remote Sensing of the Environment*, 74, 229–239.
- Errebhi, M., Rosen, C. J., Gupta, S. C., & Birong, D. E. (1998). Potato yield response and nitrate leaching as influenced by nitrogen management. *Agronomy Journal*, 90, 10–15.
- Ferguson, R. B., Hergert, G. W., Schepers, J. S., Gotway, C. A., Cahoon, J. E., & Peterson, T. A. (2002). Site-specific nitrogen management of irrigated maize: Yield and soil residual nitrate effects. *Soil Science Society of America Journal*, 66, 544–553.
- Gates, D. M., Keegan, H. J., Schleter, J. C., & Weidner, V. R. (1965). Spectral properties of plants. *Applied Optics*, 4, 11–20.
- Gitelson, A. A., Gritz, Y., & Merzlyak, M. N. (2003). Relationships between leaf chlorophyll content and spectral reflectance and algorithms for non-destructive chlorophyll assessment in higher plant leaves. *Journal of Plant Physiology*, 160, 271–282.
- Gitelson, A. A., & Merzlyak, M. N. (1997). Remote estimation of chlorophyll content in higher plant leaves. *International Journal of Remote Sensing*, 18, 2691–2697.
- Haboudane, D., Miller, J. R., Pattey, E., Zarco-Tejada, P. J., & Strachan, I. B. (2004). Hyperspectral vegetation indices and novel algorithms for predicting green LAI of crop canopies: Modeling and validation in the context of precision agriculture. *Remote Sensing of Environment*, 90, 337–352.
- Haboudane, D., Miller, J. R., Tremblay, N., Zarco-Tejada, P. J., & Dextraze, L. (2002). Integrated narrow-band vegetation indices for prediction of crop chlorophyll content for application to precision agriculture. *Remote Sensing of Environment*, 81, 416–426.
- Herrmann, I., Karnieli, A., Bonfil, D. J., Cohen, Y., and Alchanatis, V. (2009). SWIR-based spectral indices for assessing nitrogen content in potato fields. *International Journal of Remote Sensing*. (In press).
- Hu, B. X., Qian, S. E., Haboudane, D., Miller, J. R., Hollinger, A. B., Tremblay, N., et al. (2004). Retrieval of crop chlorophyll content and leaf area index from decompressed hyperspectral data: The effects of data compression. *Remote Sensing of Environment*, 92, 139–152.

- Jain, N., Ray, S. S., Singh, J. P., & Panigrahy, S. (2007). Use of hyperspectral data to assess the effects of different nitrogen applications on a potato crop. *Precision Agriculture*, 8, 225–239.
- Meyer, R. D., & Marcum, D. B. (1998). Potato yield, petiole nitrogen, and soil nitrogen response to water and nitrogen. *Agronomy Journal*, 90, 420–429.
- National Potato Council (NPC). (2006). *Potato statistical yearbook, 2006–2007*. Washington, DC: National Potato Council.
- Ollinger, S. V., Smith, M. L., Martin, M. E., Hallett, R. A., Goodale, C. L., & Aber, J. D. (2002). Regional variation in foliar chemistry and N cycling among forests of diverse history and composition. *Ecology*, 83, 339–355.
- Pimstein, A., Karnieli, A., & Bonfil, D. J. (2007). Wheat and maize monitoring based on ground spectral measurements and multivariate data analysis. *Journal of Applied Remote Sensing*, 1, 013530 (On-line journal).
- Rondeaux, G., Steven, M. D., & Baret, F. (1996). Optimization of soil-adjusted vegetation indices. *Remote Sensing of Environment*, 55, 95–107.
- Shenk, J., & Westerhaus, M. (1991). Population structuring of near infrared spectra and modified partial least squares regression. *Crop Science*, 31, 1548–1555.
- Shock, C. C., Pereira, A. B., & Eldredge, E. B. (2007). Irrigation best management practices for potato. *American Journal of Potato Research*, 84, 29–37.
- Smith, M. L., Ollinger, S. V., Martin, M. E., Aber, J. D., Hallett, R. A., & Goodale, C. L. (2002). Direct estimation of aboveground forest productivity through hyperspectral remote sensing of canopy nitrogen. *Ecological Applications*, 12, 1286–1302.
- Strachan, I. B., Pattey, E., & Boisvert, J. B. (2002). Impact of nitrogen and environmental conditions on corn as detected by hyperspectral reflectance. *Remote Sensing of Environment*, 80, 213–224.
- Thomas, J. R., & Gausman, H. W. (1977). Leaf reflectance vs. leaf chlorophyll and carotenoid concentrations for eight crops. *Agronomy Journal*, 69, 799–802.
- Townsend, P. A., Foster, J. R., Chastain, R. A., & Currie, W. S. (2003). Application of imaging spectroscopy to mapping canopy nitrogen in the forests of the central Appalachian Mountains using hyperion and AVIRIS. *IEEE Transactions on Geoscience and Remote Sensing*, 41, 1347–1354.
- Tso, B., & Mather, P. (2001). *Classification methods for remotely sensed data* (356 pp). Boca Raton, FL: CRC.
- Van-Alphen, B. J., & Stoorvogel, J. J. (2000). A functional approach to soil characterization in support of precision agriculture. *Soil Science Society of America Journal*, 64, 1706–1713.
- Vincini, M., & Frazzi, E. (2009). Sensitivity of narrow and broad-band vegetation indices to leaf chlorophyll concentration in planophile crops canopies. In E. J. van Henten, D. Goense, & C. Lokhorst (Eds.), *Precision agriculture '09* (pp. 39–45). Wageningen: Wageningen Academic Publishers.
- Vincini, M., Frazzi, E., & D'Alessio, P. (2008). A broad-band leaf chlorophyll vegetation index at the canopy scale. *Precision Agriculture*, 9, 303–319.
- Westermann, D. T., & Kleinkopf, G. E. (1985). Nitrogen requirements of potatoes. *Agronomy Journal*, 77, 616–621.
- Zakaluk, R., & Ranjan, R. S. (2007). Artificial neural network modelling of leaf water potential for potatoes using RGB digital images: a greenhouse study. *Potato Research*, 49, 255–272.
- Zarco-Tejada, P. J., Berjon, A., Lopez-Lozano, R., Miller, J. R., Martin, P., Cachorro, V., et al. (2005). Assessing vineyard condition with hyperspectral indices: leaf and canopy reflectance simulation in a row-structured discontinuous canopy. *Remote Sensing of Environment*, 99, 271–287.
- Zebarth, B. J., & Rosen, C. J. (2007). Research perspective on nitrogen BMP development for potato. *American Journal of Potato Research*, 84, 3–18.